



HAL
open science

On the rise times in FU Orionis events

Elisabeth M. A. Borchert, Daniel J. Price, Christophe Pinte, Nicolás Cuello

► **To cite this version:**

Elisabeth M. A. Borchert, Daniel J. Price, Christophe Pinte, Nicolás Cuello. On the rise times in FU Orionis events. *Monthly Notices of the Royal Astronomical Society: Letters*, 2022, 510, pp.L37-L41. 10.1093/mnrasl/slab123 . insu-03705376

HAL Id: insu-03705376

<https://insu.hal.science/insu-03705376>

Submitted on 12 Apr 2023

HAL is a multi-disciplinary open access archive for the deposit and dissemination of scientific research documents, whether they are published or not. The documents may come from teaching and research institutions in France or abroad, or from public or private research centers.

L'archive ouverte pluridisciplinaire **HAL**, est destinée au dépôt et à la diffusion de documents scientifiques de niveau recherche, publiés ou non, émanant des établissements d'enseignement et de recherche français ou étrangers, des laboratoires publics ou privés.

On the rise times in FU Orionis events

Elisabeth M. A. Borchert ¹★, Daniel J. Price ¹, Christophe Pinte ^{1,2} and Nicolás Cuello ²

¹*School of Physics and Astronomy, Monash University, Clayton, VIC 3800, Australia*

²*Univ. Grenoble Alpes, CNRS, IPAG/UMR 5274, F-38000 Grenoble, France*

Accepted 2021 November 22. Received 2021 November 10; in original form 2021 October 20

ABSTRACT

We examine whether stellar flyby simulations can initiate FU Orionis outbursts using 3D hydrodynamics simulations coupled to live Monte Carlo radiative transfer. We find that a flyby where the secondary penetrates the circumprimary disc triggers a 1–2 yr rise in the mass accretion rate to $10^{-4} M_{\odot} \text{ yr}^{-1}$ that remains high ($\gtrsim 10^{-5} M_{\odot} \text{ yr}^{-1}$) for more than a hundred years, similar to the outburst observed in FU Ori. Importantly, we find that the less massive star becomes the dominant accretor, as observed.

Key words: hydrodynamics – methods: numerical – protoplanetary discs – stars: protostars – stars: variables: T Tauri, Herbig Ae/Be.

1 INTRODUCTION

The year was 1936. Over the course of the year, a previously unremarkable 16th magnitude star in Orion brightened by 6 magnitudes. FU Ori has remained bright ever since. Many explanations have been proposed, but none completely explains the phenomenon.

FU Ori is now the leading head of a class of low-mass, pre-main-sequence stars that experience sudden increases in brightness over a short period of time (Herbig 1966, 1977). Since the first detection, a number of objects have been classed as FU Orionis objects (FUors) based upon similar observed outbursts, or their spectral characteristics (see review by Hartmann & Kenyon 1996). The outbursts, while yet to be explained, are thought to be an important aspect of the star formation process, leading to sudden bursts in the accretion rate (Hartmann & Kenyon 1996).

Reasonable explanations for the outbursts range from disc thermal instability (Lin, Papaloizou & Faulkner 1985; Clarke, Lin & Pringle 1990; Bell et al. 1995) to binary interactions (Bonnell & Bastien 1992; Reipurth & Aspin 2004), or perhaps a combination of the two. Binary interaction seems probable in FU Ori, in particular after Wang et al. (2004) first resolved FU Ori N and S. The binary was characterized further by Reipurth & Aspin (2004) and Beck & Aspin (2012). More recent observations in scattered light (Liu et al. 2016; Takami et al. 2018) and most recently with the Atacama Large Millimetre/submillimetre Array (ALMA; Pérez et al. 2020) show strong perturbations in the disc, suggesting past binary interactions, though other interpretations are possible (cf. Takami et al. 2018). Similar disturbed morphologies have been observed with ALMA around other FUors (Hales et al. 2015) but have been interpreted as conical outflows (Ruíz-Rodríguez et al. 2017a; Zurlo et al. 2017).

In this letter, we consider the hypothesis of FU Ori-like outbursts being induced by a stellar flyby (Pfalzner 2008; Cuello et al. 2019, 2020; Vorobyov et al. 2021). Flyby scenarios have previously been discounted due to a paucity of detected close companions (1/3; Green et al. 2016) as well as their inability to maintain outbursts for 100 yr

(Clarke et al. 1990). However, companions are easily obscured by disturbed material.

Importantly, observations have shown that in FU Ori the ‘primary’ is not actually the primary. FU Ori N, the more luminous star, is the lower mass star (0.3–0.6 M_{\odot} ; Zhu et al. 2007; Pérez et al. 2020). FU Ori N is the star in outburst, with $\dot{M} \approx 3.8 \times 10^{-5} M_{\odot} \text{ yr}^{-1}$ (Pérez et al. 2020). FU Ori S, the less luminous star, is the higher mass star (1.2 M_{\odot}) and accretes at a normal rate, $\dot{M} \approx (2\text{--}3) \times 10^{-8} M_{\odot} \text{ yr}^{-1}$ (Beck & Aspin 2012). We therefore should not be trying to trigger an outburst in the primary disc. Rather, *the outburst needs to occur around the perturber*. Vorobyov et al. (2021) reproduced such outbursts with retro- and prograde disc-penetrating flybys, though not yet on time-scales comparable to FUors.

Our main aim is to test whether a stellar flyby that penetrates the disc can produce a fast-rising but long-lasting outburst. We build on the flyby simulations performed by Cuello et al. (2019) but with on-the-fly live radiative transfer calculations. While our simulations are motivated by observations in FU Ori, we have not attempted a detailed reconstruction.

2 METHODS

We performed 3D radiation hydrodynamic simulations with the smoothed particle hydrodynamics (SPH) code PHANTOM (Price et al. 2018) coupled to the Monte Carlo radiative transfer code MCFOST (Pinte et al. 2006, 2009). Our simulations build on previous flyby simulations performed by Cuello et al. (2019) with two key differences. First, rather than prescribing a fixed radial temperature profile as in Cuello et al. (2019), we updated the temperature live during the calculation by calling MCFOST on the fly at set intervals. This allowed us to compute disc temperature profiles self-consistently, even if there were discs formed around both stars. Secondly, we included a contribution from the mass accretion rate in the stellar luminosity used to irradiate the disc(s) during the temperature calculations in MCFOST. This allowed for the possibility of thermal feedback from the enhanced accretion rate induced by the flyby. We assumed that the gas and dust temperatures were equal when updating the temperature

* E-mail: elisabeth.borchert@monash.edu

from MCFOST in the SPH calculations. This assumption is valid except in the low-density upper atmosphere (e.g. Woitke, Kamp & Thi 2009), and does not impact our estimated accretion rates. Our method implicitly assumes radiative equilibrium between the stellar radiation and the gas at all times.

We used the same set-up as in Cuello et al. (2019), using a prograde flyby at an angle of $\beta = 45^\circ$ (as this showed the highest accretion outburst), and flip the whole system for presentation in order to match observed disc rotation in FU Ori. The mass of the primary was set to $1.2 M_\odot$ and the perturber mass to $0.6 M_\odot$, based on observational estimates in FU Ori (Zhu et al. 2007; Pérez et al. 2020). Stars were treated as sink particles with an accretion radius of 0.5 au. Their initial separation was set to 10 times the periastron distance on a parabolic orbit. The primary was set-up with a surrounding disc of $0.02 M_\odot$, an inner radius of 1 au, an outer radius at 50 au, and an initial surface density profile $\Sigma(r) \propto r^{-1}$. For the purposes of placing the particles, we assumed an initial $H/R = 0.05(R/1 \text{ au})^{1/4}$, though this is free to change based on the temperature obtained from the radiative transfer code. As usual, we use the SPH shock viscosity to mimic a disc viscosity (Lodato & Price 2010) with $\alpha_{\text{av}} = 0.22$ giving $\alpha_{\text{disc}} \approx 0.005$, appropriate to a weakly ionized disc. Our simulations were performed with 10^6 SPH particles, initially in the primary disc.

We performed a set of simulations, changing the periastron distance while keeping the above parameters fixed. We used distances ranging from 5 to 50 au in 5 au increments plus two additional simulations at 60 and 100 au. The time interval to call MCFOST was set to 1/100 of the time it takes the stellar flyby to reach the same separation past periastron as in the initial conditions at 10 times periastron (computed using Barker’s equation; Cuello et al. 2019), i.e. 100 calls over the course of the simulation – 50 on the approach to periastron and 50 after.

For each sink particle, we computed the time-averaged mass accretion rate \dot{M} since the previous call to MCFOST. Using this, we calculated the accretion luminosity (Shakura & Sunyaev 1973) and temperature as

$$L_{\text{acc}} = \frac{1}{2} \frac{GM_\star \dot{M}}{R_\star} \quad \text{and} \quad T_{\text{acc}} = \left(\frac{L_{\text{acc}}}{4\pi\sigma R_\star^2} \right)^{1/4}, \quad (1)$$

with the Stefan Boltzmann constant σ . The stellar radii R_\star and effective temperatures are calculated in MCFOST from the sink particle masses M_\star using the 3 Myr isochrone from Siess, Dufour & Forestini (2000), which leads to $R_\star = 1.4 R_\odot$ and $T_{\text{eff}} = 3882 \text{ K}$. We then selected the closest stellar spectra in the ‘NextGen’ data base (Hauschildt, Allard & Baron 1999). The accretion luminosity is emitted uniformly from the stellar surface (on top of the stellar luminosity) with a blackbody spectrum with $T = T_{\text{acc}}$.

3 RESULTS

Fig. 1 shows column density in our simulation with $r_p = 20 \text{ au}$, 35.5 yr before and 11.5 and 97.5 yr after periastron (left to right, respectively) and from two perspectives (top and bottom rows, respectively). The rings in the primary disc are an artefact from the initial response to the inner disc boundary condition.

Fig. 2 shows density normalized temperature maps (line-of-sight integral of ρT divided by line-of-sight integral of ρ) for the same snapshots as in Fig. 1. During the time of closest approach, temperatures around the perturber can be seen to reach up to $\sim 1580 \text{ K}$. The maximum temperatures occur around the perturber during the process of penetrating the disc (middle panel).

While travelling through the primary disc, the secondary experiences a sudden spike in mass accretion, shown by the orange line

in Fig. 3. This rise begins when the secondary passes through the primary disc and captures material (bottom panel of Fig. 1). Before interacting with the disc, our secondary does not accrete mass as there is no disc surrounding it. We observe a fast rise of the mass accretion rate on to the secondary in all simulations where the secondary penetrates the disc. The amplitude of the outburst decreases with increasing periastron distance. At $r_p = 60 \text{ au}$, when the perturber no longer penetrates the primary disc, there remains a small accretion burst on the secondary, though of a considerably smaller magnitude and duration compared to penetrating encounters (less than half an order of magnitude increase in \dot{M}_2 over the pre-burst \dot{M}_1 at $r_p = 60 \text{ au}$ compared to ~ 2 orders of magnitude for closer perturbers). The only simulations where we observed no outburst on the secondary used a periastron distance of 100 au. At such a distance, the secondary disturbs the primary disc but does not capture a significant amount of material, giving $\dot{M}_2 \lesssim 10^{-8} M_\odot \text{ yr}^{-1}$.

The dark blue line in Fig. 3 shows that, as the secondary experiences an accretion burst while passing through the disc, the primary also experiences a small burst in mass accretion, visible as a small spike at about 190 yr (11.5 yr post-pericentre). This burst is slightly delayed compared to the burst in the secondary, and with a smaller amplitude. The primary outburst is caused by shocks in the disc excited by the perturber, which travel inwards to create the burst in accretion on the primary. Up to periastron distances of $r_p = 40 \text{ au}$, the amplitude of the outburst in the primary sits at about an order of magnitude above the pre-flyby mass accretion rate. The amplitude of the mass accretion rate for the primary decreases for more distant flybys and disappears completely when the secondary does not penetrate the disc.

Fig. 3 shows that \dot{M} of the secondary rises by more than two orders of magnitude over a short time interval (rise time of a few years). This is an order of magnitude shorter than the orbital time-scale of the primary disc at the perturber location ($\approx 80 \text{ yr}$).

In the top panel of Fig. 4, we show the rise times of different simulations as a function of periastron distance for our set of simulations. The bottom panel shows the maximum mass accretion rate of the outburst as a function of periastron distance. We defined the rise time as the time it takes for the accretion rate to reach the maximum accretion rate from the average accretion rate of the primary before the outburst. That is, the time it takes for the perturber’s accretion rate to go from the primary’s pre-burst accretion rate ($\sim 5 \times 10^{-7} M_\odot$) to the peak accretion ($\sim 2 \times 10^{-4} M_\odot$). The dark blue shows the rise time in the primary and the orange the rise time in the secondary. We included a horizontal line showing the rise time we measured the same way from the observed FU Ori light curve (fig. 3 in Hartmann & Kenyon 1996). In general, we see a trend of longer rise times for increasing periastron distances. For $r_p \geq 35 \text{ au}$, we observe a drop in the rise times of the secondary from the previously observed trend. At this point, the amplitude of the outburst reduces from ≥ 2 orders of magnitude to < 2 orders of magnitude.

We can understand the rapid time-scale as follows: While the primary receives its accretion outburst from inward evolution of disc disturbances, the secondary goes into outburst when penetrating the disc of the primary, capturing material and accreting rapidly due to direct cancellation of angular momentum. We model the secondary outburst with a theoretical relation by assuming the perturber at speed $v = \sqrt{2GM/r_p}$ passes through a certain distance $L(r_p)$ of the disc, shown as the dotted line in Fig. 4. This leads to the theoretical rise time of

$$t_{\text{rise}} = \frac{L(r_p)}{\sqrt{2GM/r_p}}, \quad (2)$$

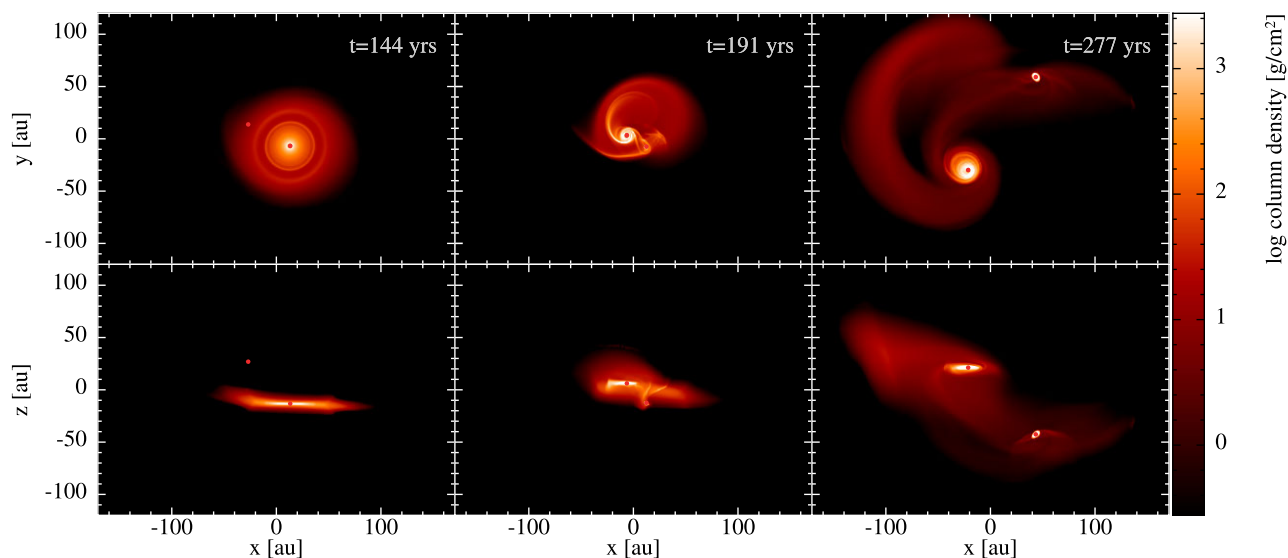


Figure 1. Column density of a stellar flyby at $r_p = 20$ au. The top row shows a top view and the bottom row a side view. Each column shows the same snapshots from the simulation, giving a visual representation ~ 35.5 yr before and ~ 11.5 and ~ 97.5 yr after periastron (left to right). The red dots in the plots indicate the location of the stars. The secondary can be seen to grab material from the primary disc that becomes a circumsecondary disc.

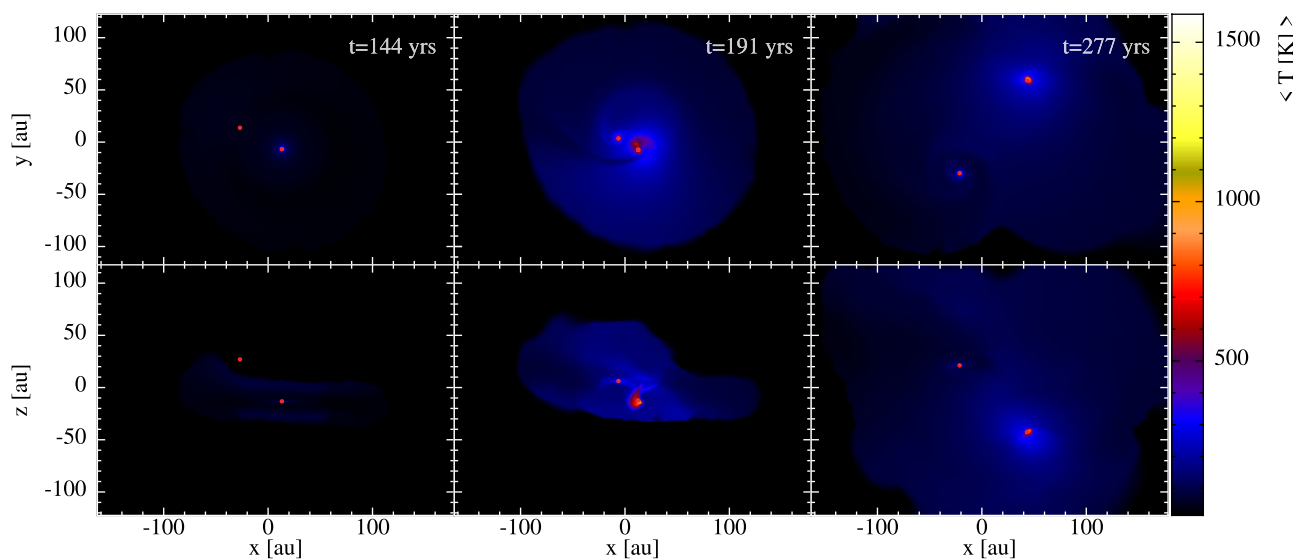


Figure 2. Normalized temperature plot for the same views and snapshots as in Fig. 1. The highest normalized temperatures reach ~ 1580 K. After the perturber passes through the disc, the right-hand column shows that the circumsecondary disc remains hotter than the disc surrounding the primary.

with the total mass of both stars M . The length $L(r_p)$ used for the theoretical line in Fig. 4 corresponds to $L(r_p) = 5.7H$, with $H = r_p \times (H/R)_{R=r_p}$. Given the primary disc aspect ratio and the flaring index, this leads to the following dependence between the rise time and the periastron distance:

$$t_{\text{rise}} \propto r_p^{5/4}. \quad (3)$$

This relation holds when the perturber passes through the bulk of the disc. We can see in Fig. 4 that the results start to deviate significantly when the periastron distance approaches the outer edge of the disc. Fig. 4 shows that deviations from the theoretical trend occur for periastron distances above 30 au due to tidal truncation.

The accretion burst seen in Fig. 3 is sustained for more than 100 yr by ongoing infall on to the circumsecondary disc from the surroundings.

4 DISCUSSION

The main objection to binary interactions as the origin for FU Orionis outbursts relates to the fast rise time. According to Hartmann & Kenyon (1996), ‘To explain the fastest rise times of a year, the eruption must involve disc regions smaller than one au [because disc evolution will occur on timescales much longer than an orbital period (Pringle 1981)]’. This makes the false assumption that the primary disc goes into outburst. This is not what was observed in FU Ori, where the more luminous star is actually the low-mass star,

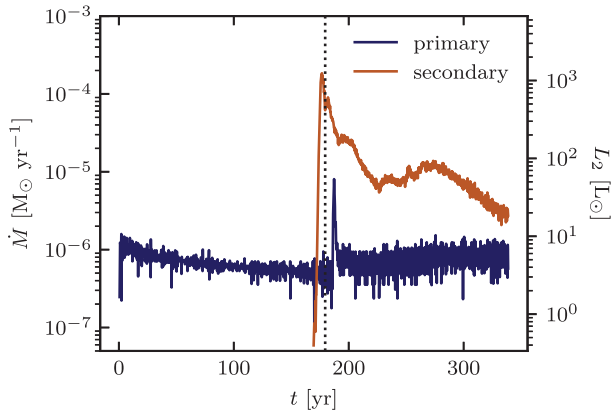


Figure 3. Time evolution of the accretion rate of the primary (dark blue) and the secondary (orange) from the simulation with $r_p = 20$ au. The right axis shows the accretion luminosity of the secondary. Dotted line indicates periastron at ≈ 179.5 yr. We see an outburst in the secondary (happening from 171 to 175 yr), while the primary only experiences a small burst. Furthermore, the accretion rate, while not maintained at the maximum, continues at one to two orders of magnitude higher than what was observed pre-flyby in the primary.

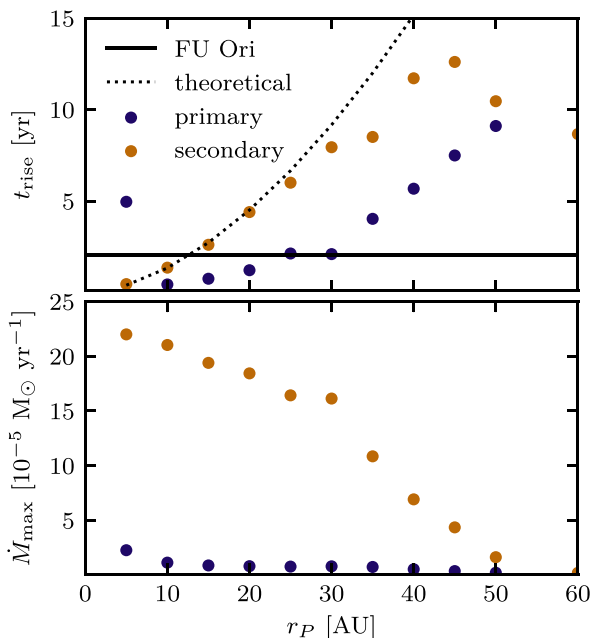


Figure 4. Rise time (top) and maximum mass accretion rate (bottom) for different periastron distances. Dark blue is for the primary star while orange is for the secondary. Horizontal line shows the rise time we calculated for FU Ori from its light curve (see fig. 3 in Hartmann & Kenyon 1996) in the top. The dotted line shows a theoretical estimate for the rise time of the stellar flyby following equation (2).

i.e. the perturber (Reipurth & Aspin 2004; Wang et al. 2004; Beck & Aspin 2012; Pérez et al. 2020).

In our simulations, it is indeed the secondary that goes into a sustained outburst. The luminosity of our secondary exceeds $100 L_{\odot}$ for 40 yr before continuing at about $40 L_{\odot}$. The primary does *not* go into a sustained outburst, although a spike in \dot{M}_1 occurs shortly after periastron. This also agrees with observations: FU Ori S, the more massive star, accretes at a normal rate with an unexceptional luminosity of $\sim 2\text{--}3 L_{\odot}$ (Beck & Aspin 2012).

The rise times of our outbursts are on a time-scale that is comparable to the fastest time-scales observed in FUors, e.g. in FU Ori and V1057 Cyg (see table 1 in Hartmann & Kenyon 1996). This is visible in Fig. 4, where we reproduce the rise time of FU Ori for a prograde stellar flyby at 10–15 au periastron distance. With our secondary going into outburst, we do not require the interaction to happen at a distance of less than 1 au. The main requirement for the secondary to erupt is that the secondary penetrates the primary disc at periastron. The trend seen in Fig. 3 is in line with the findings in Vorobyov et al. (2021), except their rise time is of the order of ~ 1 kyr, longer than those associated with FU Orionis outbursts. Closer flybys result in a faster and higher rise in the mass accretion rate. Wider separation passages may explain longer rise times in other FUors (e.g. V1515 Cyg). Our findings and the results from Vorobyov et al. (2021) show that flybys can trigger either fast or slow accretion bursts depending on whether or not the perturber penetrates the disc, respectively.

Our models of the secondary going into outburst may also explain the distinctive optical and near-infrared characteristics of FUors (Hartmann & Kenyon 1996; Beck & Aspin 2012; Connelley & Reipurth 2018). First, they all have reflection nebulae (Herbig 1977; Goodrich 1987). Secondly, in near-infrared FUors look like K–M giants, while optical observations suggest effective temperatures of 6500–7200 K and low surface gravities. We can explain this because our secondary is a low-mass star (K–M) with a very high surface temperature, up to 10^4 K depending on our assumed radius.

ALMA observations of FU Ori revealed direct evidence for binary interactions (Zurlo et al. 2017; Cieza et al. 2018; Pérez et al. 2020; Kóspál et al. 2021). In particular, CO line observations have revealed distinct blue- and redshifted velocities corresponding to expanding ‘shells or rings’. These flows, previously interpreted as conical outflows (Ruíz-Rodríguez et al. 2017a,b; Zurlo et al. 2017), are naturally explained by line-of-sight motions of our interacting discs post-periastron. Our models show both blue- and redshifted line-of-sight motions of the order of $5\text{--}20$ km s^{-1} (see e.g. synthetic line observations in Cuello et al. 2020).

Instead of binary interactions, disc instabilities have previously been the favoured scenario for FU Orionis outbursts (Bell et al. 1995). In our simulations, we triggered an outburst on the observed time-scale that is maintained for more than 100 yr without the need for thermal instability. Fig. 2 shows the temperature evolution in our flyby scenario. Through the use of on-the-fly radiative transfer calculations, we were able to model the changes in disc temperature. Around the time of periastron, temperatures in the circumsecondary disc increase significantly. The disc temperature reaches up to ~ 1580 K close to the perturber. These temperatures, while high, are still considerably below the temperatures required to initiate thermal instability. We therefore demonstrate that FU Orionis outbursts are possible without the need for thermal instability.

While the simulations do not reach the temperatures required for thermal instability, we do observe temperatures rising above 1500 K (see middle column in Fig. 2). Dust should sublimate at this point as the temperatures are above 1000 K. Preliminary tests where we tried removing dust at temperatures above 1000 K did not change our results and thus we did not account for this in our final models. Interestingly, such rapid heating of the disc with dust melting could possibly explain the existence of chondrules in our Solar system, where dynamical evidence for a past flyby exists (Pfalzner et al. 2018). Flash heating occurs to some extent around both stars, so evidence for similar heating in the Solar system does not necessarily imply that our Sun was the perturber.

In our simulations, we have not attempted a detailed reconstruction of the close encounter in FU Orionis. This is the likely reason we are not yet able to maintain the outburst exactly as seen in FU Ori. We have cases though where the secondary maintains a higher mass accretion rate than that of the primary (at least an order of magnitude for more than 100 yr). One such example is shown in Fig. 3. Sustained outbursts occur when the secondary captures material to form a circumsecondary disc with subsequent ongoing infall. One such case is the simulation presented in Figs 1 and 3, with the perturber disc visible in the right-hand column in Fig. 1.

We did not include magnetic fields in our calculations. Doing so would enable us to launch $\gtrsim 200 \text{ km s}^{-1}$ jets from the inner disc, as seen in several FUors (e.g. V1057 Cyg; Levreault 1988).

Our simulations provide an explanation for single FU Orionis outburst events. As we assumed a penetrating unbound stellar flyby, our secondary will only pass through periastron once, leading to one outburst. There are FUors that have experienced multiple outbursts (e.g. Z CMA) that have previously been predicted by bound binary interactions (Bonnell & Bastien 1992).

5 CONCLUSIONS

We performed a series of numerical experiments of thermal feedback in 3D simulations of stellar flybys. We have been able to reproduce three key features of the observed outburst in FU Ori.

- (i) We were able to reproduce a fast accretion rise as seen in FU Ori, with perturbers that penetrate the disc (no thermal instability).
- (ii) The mass accretion rate of the secondary continues at a higher level (one to two orders of magnitude) to what it had been pre-flyby for the primary for more than 100 yr. This occurs because of ongoing infall from the environment on to the circumsecondary disc.
- (iii) Our simulations further show the observed phenomenon of the lower mass star going into outburst, as is the case in FU Ori.

It would be interesting to explore whether different stellar flybys at different angles, with different disc properties and accretion radii or a disc around the perturber, are able to sustain the outburst at a higher amplitude for longer. In preliminary attempts at disc–disc flybys, we find more sustained outbursts depending on the relative initial disc orientations. Another important follow-up should be to create synthetic observations and light curves in order to reconstruct what was observed in FU Ori in 1937.

ACKNOWLEDGEMENTS

We thank our referee for a constructive and timely report and Iain Hammond, Evgeni Grishin, and Giuseppe Lodato for useful discussions. DJP thanks Agnes Kóspál and Peter Ábrahám for useful discussions following the ‘Great Barriers in Planet Formation’ conference in 2019. EMAB acknowledges an Australian Government Research Training Program (RTP) and a Monash International Tuition Scholarship. We acknowledge Australian Research Council grants FT170100040 and DP180104235. NC acknowledges support from the European Union’s Horizon 2020 research and innovation programme under the Marie Skłodowska-Curie grant agreement No 210021. We used Ozstar and Gadi via the National Computing Infrastructure/Swinburne University. We used SPLASH (Price

2007), MATPLOTLIB (Hunter 2007), NUMPY (Harris et al. 2020), and CMASHER (van der Velden 2020).

DATA AVAILABILITY

PHANTOM¹ and MCFOST² are publicly available and the simulation set-up and data underlying this article will be shared on request.

REFERENCES

- Beck T. L., Aspin C., 2012, *AJ*, 143, 55
 Bell K. R., Lin D. N. C., Hartmann L. W., Kenyon S. J., 1995, *ApJ*, 444, 376
 Bonnell I., Bastien P., 1992, *ApJ*, 401, L31
 Cieza L. A. et al., 2018, *MNRAS*, 474, 4347
 Clarke C. J., Lin D. N. C., Pringle J. E., 1990, *MNRAS*, 242, 439
 Connelley M. S., Reipurth B., 2018, *ApJ*, 861, 145
 Cuello N. et al., 2019, *MNRAS*, 483, 4114
 Cuello N. et al., 2020, *MNRAS*, 491, 504
 Goodrich R. W., 1987, *PASP*, 99, 116
 Green J. D. et al., 2016, *ApJ*, 830, 29
 Hales A. S. et al., 2015, *ApJ*, 812, 134
 Harris C. R. et al., 2020, *Nature*, 585, 357
 Hartmann L., Kenyon S. J., 1996, *ARA&A*, 34, 207
 Hauschildt P. H., Allard F., Baron E., 1999, *ApJ*, 512, 377
 Herbig G. H., 1966, *Vistas Astron.*, 8, 109
 Herbig G. H., 1977, *ApJ*, 217, 693
 Hunter J. D., 2007, *Comput. Sci. Eng.*, 9, 90
 Kóspál Á. et al., 2021, *ApJS*, 256, 30
 Levreault R. M., 1988, *ApJ*, 330, 897
 Lin D. N. C., Papaloizou J., Faulkner J., 1985, *MNRAS*, 212, 105
 Liu H. B. et al., 2016, *Sci. Adv.*, 2, e1500875
 Lodato G., Price D. J., 2010, *MNRAS*, 405, 1212
 Pérez S. et al., 2020, *ApJ*, 889, 59
 Pfalzner S., 2008, *A&A*, 492, 735
 Pfalzner S., Bhandare A., Vincke K., Lacerda P., 2018, *ApJ*, 863, 45
 Pinte C., Ménard F., Duchêne G., Bastien P., 2006, *A&A*, 459, 797
 Pinte C. et al., 2009, *A&A*, 498, 967
 Price D. J., 2007, *Publ. Astron. Soc. Aust.*, 24, 159
 Price D. J. et al., 2018, *Publ. Astron. Soc. Aust.*, 35, e031
 Pringle J. E., 1981, *ARA&A*, 19, 137
 Reipurth B., Aspin C., 2004, *ApJ*, 608, L65
 Ruíz-Rodríguez D. et al., 2017a, *MNRAS*, 466, 3519
 Ruíz-Rodríguez D. et al., 2017b, *MNRAS*, 468, 3266
 Shakura N. I., Sunyaev R. A., 1973, *A&A*, 500, 33
 Siess L., Dufour E., Forestini M., 2000, *A&A*, 358, 593
 Takami M. et al., 2018, *ApJ*, 864, 20
 van der Velden E., 2020, *J. Open Source Softw.*, 5, 2004
 Vorobyov E. I. et al., 2021, *A&A*, 647, A44
 Wang H., Apai D., Henning T., Pascucci I., 2004, *ApJ*, 601, L83
 Woitke P., Kamp I., Thi W. F., 2009, *A&A*, 501, 383
 Zhu Z. et al., 2007, *ApJ*, 669, 483
 Zurlo A. et al., 2017, *MNRAS*, 465, 834

¹<https://github.com/danieljprice/phantom>

²<https://github.com/cpinte/mcfost>

This paper has been typeset from a $\text{\TeX}/\text{\LaTeX}$ file prepared by the author.